Journal of Sound and Vibration (2001) **242**(1), 27–46
doi:10.1006/jsvi.2000.3334, available online at http://www.idealibrary.com on IDEAL®

SIMULTANEOUS COMBINATION, PRINCIPAL PARAMETRIC AND INTERNAL RESONANCES IN A SLENDER BEAM WITH A LUMPED MASS: THREE-MODE INTERACTIONS

S. K. DWIVEDY† AND R. C. KAR

Department of Mechanical Engineering, Indian Institute of Technology, Kharagpur 721 302, *India*

(*Received* 6 *August* 1999, *and in final form* 14 *June* 2000)

The non-linear dynamics of a parametrically base-excited slender beam carrying a lumped mass with an excitation frequency nearly equal to twice the second mode natural frequency is examined. The mass and the position of the attached element are so adjusted that the system exhibits 1 : 3 : 5 internal resonance by virtue of which a combination resonance of type $\omega_1 + \omega_3$ occurs simultaneously in the system. The method of multiple scales (mms) is applied to reduce the second order temporal differential equations of motion of the system to a set of first order differential equations which is used to study the steady state, periodic, quasi-periodic and chaotic responses of the system for different control parameters, namely, frequency and amplitude of base excitation, damping, internal detuning, etc. The results of perturbation analysis are compared with those obtained by numerically integrating the original temporal equations of motion. Poincaré section and Lyapunov exponents are used to characterize the chaotic responses.

1. INTRODUCTION

A slender beam with an attached mass can find application in the study of vibration [1–12] of the appendages of space crafts, manipulator arms, high-speed machinery, high rises and many other structural elements. For some amplitude and frequency of base motion, the system is subjected to parametric excitation and when the response amplitude becomes large, non-linearities begin to affect the motion and hence one cannot apply the usual linear analysis to obtain the resonant behaviour. Also, for some location and dimension of the attached mass, the natural frequencies of the system are commensurable giving rise to internal resonances [11–13] making the analysis of the system very complex and time consuming.

Though there are a number of studies available on the base-excited cantilever beam with an attached mass, most of them deal with the determination of natural frequencies and linear mode shapes [1–5] and some determine the trivial state stability boundary and non-linear response of the system with single-mode approximation [6–10]. Zavodney and Nayfeh [10] studied theoretically as well as experimentally the non-linear response of a slender beam carrying a lumped mass to a principal parametric excitation. They used single-mode approximation as the chosen physical parameters do not yield internal resonance. The present authors addressed the same system of Zavodney and Nayfeh and

†Presently at Mechanical Engineering Department, Indian Institute of Technology, Guwahati 781 001, India.

0022-460X/01/160027 + 20 $35.00/0

found internal resonance conditions [11–13] for certain mass and position of the attached element. In these studies, the internal resonance of 1 : 3 was considered along with principal parametric [11] and combination parametric [12, 13] resonances, and many interesting fixed-point, periodic, quasi-periodic and chaotic responses were obtained using perturbation techniques.

For a general review of literature for parametrically excited system one may refer the texts of Nayfeh and Mook [14], Szemplińska-Stupnica [15] and Cartmell [16] and for the analysis of dynamical systems the texts by Nayfeh and Balachandran [17], Iooss and Joseph [18], Chow and Hale [19] and Kuznetsov [20].

As the importance of internal resonance is well established in the non-linear systems, many researchers studied two-degree-of-freedom systems with quadratic or cubic non-linearities having one–one, one–two, one–three type of internal resonances [11–23] for principal and/or combination parametric resonances. Due to the complexity in the analysis, most of the studies in non-linear systems are limited to two degrees of freedom and a very few studies are available for systems with three-mode interactions [24–30].

In the present paper, the parametrically excited cantilever beam with a lumped mass having cubic non-linearities of geometrical and inertial type is analyzed to obtain the non-linear responses when it is excited at a frequency nearly twice that of the second-mode natural frequency. The system parameters are so chosen that 1 :3 : 5 internal resonances are exhibited. By virtue of this internal resonance, a simultaneous combination resonance of sum type occurs in the system. The method of multiple scales (mms) is used to study the fixed-point, periodic, quasi-periodic and chaotic responses of the system for various control parameters.

2. ANALYSIS

The temporal equation of motion of a uniform cantilever beam of length L carrying a mass m at an arbitrary position d from the fixed end (Figure 1) subjected to base motion $z = Z_0 \cos \Omega t$ in the non-dimensional form can be given by [11]

$$\ddot{u}_n + 2\varepsilon\zeta_n\dot{u}_n + \omega_n^2 u_n - \varepsilon \sum_{m=1}^{\infty} f_{nm} u_m \cos(\phi\tau) + \varepsilon \sum_{k=1}^{\infty}\sum_{l=1}^{\infty}\sum_{m=1}^{\infty} \times \{\alpha_{klm}^n u_k u_l u_m + \beta_{klm}^n u_k \dot{u}_l \dot{u}_m + \gamma_{klm}^n u_k u_l \ddot{u}_m\} = 0, \tag{1}$$

where $(\dot{}) = \mathrm{d}(\ )/\mathrm{d}\tau$. u_n, ζ_n and ω_n are, respectively, the transverse displacement, damping parameter and frequency of the nth mode, f_{nm} is the forcing term in nth mode due to the modal interaction of mth mode and τ is the time. While α_{klm}^n is the geometric non-linear term, β_{klm}^n and γ_{klm}^n are the inertial non-linear terms present in the nth mode due to the modal interactions of k, l and mth modes (see Appendix of reference [11]). The small dimensionless parameter ε has been introduced as a book-keeping device to indicate the smallness of damping, non-linear terms and excitation. Due to the presence of large number of coupled non-linear terms it is practically impossible to get a closed-form solution. Hence, here a perturbation method (mms) is used to determine the approximate solutions of the system.

2.1. PHYSICAL EXAMPLE

Following Zavodney and Nayfeh [10] and keeping in view the internal resonance of 1 : 3 : 5, a metallic beam is considered with the following properties:

$$L = 125{\cdot}4 \text{ mm}, \quad I = 0{\cdot}04851 \text{ mm}^4, \quad E = 0{\cdot}20936 \times 10^6 \text{ N/mm}^2, \quad Z_r = 1 \text{ mm}$$

$$c = 0{\cdot}1 \text{ N s/mm}^2, \quad \rho = 0{\cdot}03332 \text{ gm/mm}, \quad \mu = 4{\cdot}2, \quad J = 0{\cdot}1223307, \quad \beta = 0{\cdot}24,$$

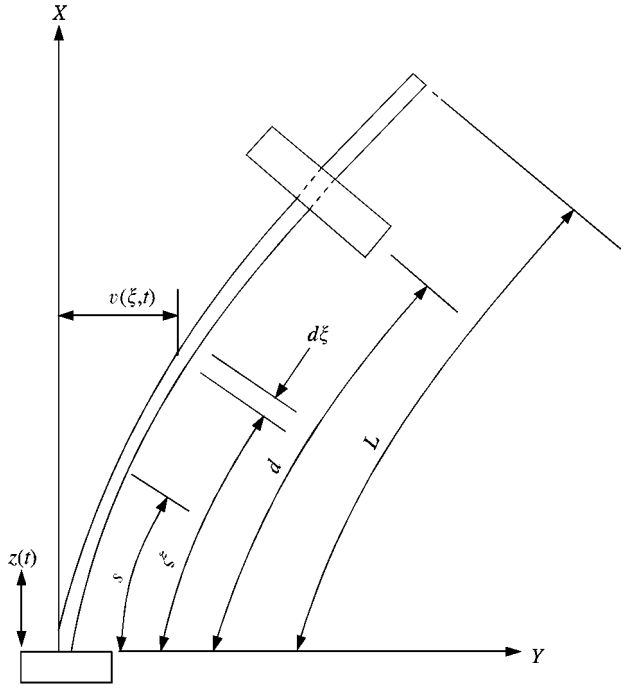

Figure 1. Base-excited cantilever beam with an attached mass.

where

$$\beta = \frac{d}{L}, \quad \tau = \theta_1 t, \quad \omega_n = \frac{\theta_n}{\theta_1}, \quad \mu = \frac{m}{\rho L}, \quad J = \frac{J_0}{\rho L^3 \lambda^2}, \quad \phi = \frac{\Omega}{\theta_1}.$$

The roots of the characteristic equation are numerically found to be $\kappa_1 = 1{\cdot}71297$, $\kappa_2 = 3{\cdot}02257, \kappa_3 = 4{\cdot}23208$ and the corresponding non-dimensional frequencies are $\omega_1 = 1$, $\omega_2 = 3{\cdot}11472$ and $\omega_3 = 5{\cdot}27647$. The book-keeping parameter ε and the scaling factor λ are taken as 0·01 and 0·1 respectively. The coefficients of damping (ζ_n), excitation (f_{nm}) and non-linear terms ($\alpha^n_{klm}, \beta^n_{klm}, \gamma^n_{klm}$) are found to be of the same order. The values of other required parameters given in Appendix A and in reference [13] are calculated to be

$$\alpha_{e11} = 0{\cdot}6604576, \quad \alpha_{e12} = -17{\cdot}9176, \quad \alpha_{e13} = 39{\cdot}64944,$$

$$\alpha_{e21} = 9{\cdot}013, \quad \alpha_{e22} = -57{\cdot}1463, \quad \alpha_{e23} = 57{\cdot}39503,$$

$$\alpha_{e31} = -97{\cdot}1194, \quad \alpha_{e32} = 0{\cdot}14784, \quad \alpha_{e33} = -211{\cdot}15,$$

$$Q_1 = 0{\cdot}2822713, \quad Q_2 = 7{\cdot}57212, \quad Q_3 = 18{\cdot}10312, \quad Q_4 = -1{\cdot}64962 \times 10^{-3},$$

$$Q_5 = -7{\cdot}70371, \quad Q_6 = 17{\cdot}62617, \quad Q_7 = 1{\cdot}97654, \quad Q_8 = 8{\cdot}60796,$$

$$f^*_{11} = 5{\cdot}37879 \times 10^{-2}, \quad f^*_{12} = 5{\cdot}48805 \times 10^{-3}, \quad f^*_{13} = 8{\cdot}80996 \times 10^{-3},$$

$$f^*_{21} = 6{\cdot}62088 \times 10^{-3}, \quad f^*_{22} = 0{\cdot}1083383, \quad f^*_{23} = 2{\cdot}20869 \times 10^{-2},$$

$$f^*_{31} = 7{\cdot}21249 \times 10^{-2}, \quad f^*_{32} = 0{\cdot}1498814, \quad f^*_{33} = 0{\cdot}1428675,$$

$$\zeta^*_1 = 4{\cdot}496846 \times 10^{-3}, \quad \zeta^*_2 = 2{\cdot}871499 \times 10^{-3}, \quad \zeta^*_3 = 1{\cdot}95911 \times 10^{-4}.$$

2.2. PERTURBATION SOLUTION

The approximate solution of equation (1) can be obtained using the method of multiple scales. Let

$$u_n(\tau;\varepsilon) = u_{n0}(T_0, T_1) + \varepsilon u_{n1}(T_0, T_1) + \cdots, \tag{2a}$$

$$T_0 = \tau, \quad T_1 = \varepsilon\tau, \quad n = 1, 2, \ldots, \infty. \tag{2b}$$

Substituting equations (2) into equation (1) and equating the coefficients of ε^0 and ε to zero, one has

$$D_0^2 u_{n0} + \omega_n^2 u_{n0} = 0, \tag{3}$$

$$D_0^2 u_{n1} + \omega_n^2 u_{n1} = -\Bigg[2\zeta_n D_0 u_{n0} + 2D_0 D_1 u_{n0} - \sum_{m=1}^{\infty} f_{nm} u_{m0} \cos\phi\tau + \sum_{klm} (\alpha_{klm}^n u_{k0} u_{l0} u_{m0} + \beta_{klm}^n u_{k0} D_0 u_{l0} D_0 u_{m0} + \gamma_{klm}^n u_{k0} u_{l0} D_0^2 u_{m0})\Bigg], \tag{4}$$

where $D_0 = \partial/\partial T_0$ and $D_1 = \partial/\partial T_1$. The solution of equation (3) is given by

$$u_{n0} = A_n(T_1)\exp(\mathrm{i}\omega_n T_0) + \mathrm{cc}, \tag{5}$$

where cc indicates the complex conjugate of the preceding terms.

For *principal parametric resonance of second mode*, the external excitation is nearly equal to twice the frequency of the second mode. Also, due to 1 : 3 : 5 internal resonances, this external frequency is approximately equal to the combination of the first- and third-mode frequencies. Hence, simultaneous principal parametric and combination resonances along with the internal resonances of 1 : 3 : 5 occur in this system. Introducing the external detuning parameter σ_1 and internal detuning parameters σ_2 and σ_3 as

$$\omega_2 = 3\omega_1 + \varepsilon\sigma_2, \qquad \omega_3 = 5\omega_1 + \varepsilon\sigma_3,$$

$$\phi = 2\omega_2 + \varepsilon\sigma_1 = \omega_1 + \omega_3 + \varepsilon(2\sigma_2 - \sigma_3 + \sigma_1) \tag{6}$$

and substituting equations (5) and (6) into equation (4) and eliminating secular terms we have

for $n = 1$,

$$2\mathrm{i}\omega_1(\zeta_1 A_1 + A_1') - \tfrac{1}{2} f_{13}\bar{A}_1 \exp\{\mathrm{i}\varepsilon(2\sigma_2 + \sigma_1 - \sigma_3)T_0\} + \sum_{j=1}^{\infty} \alpha_{e1j} A_j \bar{A}_j A_1 + Q_1 A_2 \bar{A}_1^2 \exp(\mathrm{i}\varepsilon\sigma_2 T_0) + Q_2 \bar{A}_1 \bar{A}_2 A_3 \exp\{\mathrm{i}\varepsilon(\sigma_3 - \sigma_2)T_0\} + Q_3 A_2^2 \bar{A}_3 \exp\{\mathrm{i}\varepsilon(2\sigma_2 - \sigma_3)T_0\} = 0 \tag{7}$$

for $n = 2$,

$$2\mathrm{i}\omega_2(\zeta_2 A_2 + A_2') - \tfrac{1}{2} f_{22}\bar{A}_2 \exp\{\mathrm{i}\varepsilon\sigma_1 T_0\} + \sum_{j=1}^{\infty} \alpha_{e2j} A_j \bar{A}_j A_2 + Q_4 A_1^3 \exp\{-\mathrm{i}\varepsilon\sigma_2 T_0\} + Q_5 A_3 \bar{A}_1^2 \exp\{-\mathrm{i}\varepsilon(\sigma_3 - \sigma_2)T_0\} + Q_6 A_1 \bar{A}_2 A_3 \exp\{\mathrm{i}\varepsilon(\sigma_3 - 2\sigma_2)T_0\} = 0 \tag{8}$$

for $n = 3$,

$$2\mathrm{i}\omega_3(\zeta_3 A_3 + A_3') - \tfrac{1}{3} f_{31}\bar{A}_1 \exp\{\mathrm{i}\varepsilon(2\sigma_2 + \sigma_1 - \sigma_3)T_0\} + \sum_{j=1}^{\infty} \alpha_{e3j} A_j \bar{A}_j A_3$$

$$+ Q_7 A_2 A_1^2 \exp\{\mathrm{i}\varepsilon(\sigma_2 - \sigma_3)T_0\} + Q_8 A_2^2 \bar{A}_1 \exp\{\mathrm{i}\varepsilon(2\sigma_2 - \sigma_3)T_0\} = 0 \tag{9}$$

for $n \geqslant 4$,

$$2\mathrm{i}\omega_n(\zeta_n A_n + A_n') + \sum_{j=1}^{\infty} \alpha_{enj} A_j \bar{A}_j A_n = 0, \tag{10}$$

where a prime denotes the derivative with respect to T_1. Since the higher modes ($n \geqslant 4$) are neither directly excited by external excitation nor indirectly excited by internal resonances, it can be shown from equation (10) that the response amplitudes of these modes die out due to the presence of damping. Letting $A_n = \frac{1}{2} a_n(T_1) \exp\{\mathrm{i}\beta_n(T_1)\}$ (where a_n and β_n are real) in equations (7–9) and then separating into real and imaginary parts, one obtains

$$2\omega_1(\zeta_1 a_1 + a_1') - \tfrac{1}{2} f_{13} a_3 \sin(\gamma_1 + \gamma_3) + \tfrac{1}{4} Q_1 a_1^2 a_2 \sin(3\gamma_1 - \gamma_2)$$

$$+ \tfrac{1}{4} Q_2 a_1 a_2 a_3 \sin(2\gamma_1 + \gamma_2 - \gamma_3) + \tfrac{1}{4} Q_3 a_2^2 a_3 \sin(\gamma_1 - 2\gamma_2 + \gamma_3) = 0, \tag{11a}$$

$$2\omega_1 a_1(\gamma_1' - \sigma_{e1}) - \tfrac{1}{2} f_{13} a_3 \cos(\gamma_1 + \gamma_3) + \tfrac{1}{4} Q_1 a_1^2 a_2 \cos(3\gamma_1 - \gamma_2)$$

$$+ \tfrac{1}{4} Q_2 a_1 a_2 a_3 \cos(2\gamma_1 + \gamma_2 - \gamma_3) + \tfrac{1}{4} Q_3 a_2^2 a_3 \cos(\gamma_1 - 2\gamma_2 + \gamma_3)$$

$$+ \sum_{j=1}^{3} \alpha_{e1j} a_1 a_j^2 = 0, \tag{11b}$$

$$2\omega_2(\zeta_2 a_2 + a_2') - \tfrac{1}{2} f_{22} a_2 \sin(2\gamma_2) + \tfrac{1}{4} Q_4 a_1^3 \sin(\gamma_2 - 3\gamma_1)$$

$$+ \tfrac{1}{4} Q_5 a_3 a_1^2 \sin(2\gamma_1 + \gamma_2 - \gamma_3)$$

$$+ \tfrac{1}{4} Q_6 a_1 a_2 a_3 \sin(2\gamma_2 - \gamma_1 - \gamma_3) = 0, \tag{11c}$$

$$2\omega_2 a_2(\gamma_2' - \sigma_{e2}) - \tfrac{1}{2} f_{22} a_2 \cos(2\gamma_2) + \tfrac{1}{4} Q_4 a_1^3 \cos(\gamma_2 - 3\gamma_1)$$

$$+ \tfrac{1}{4} Q_5 a_3 a_1^2 \cos(2\gamma_1 + \gamma_2 - \gamma_3) + \tfrac{1}{4} Q_6 a_1 a_2 a_3 \cos(2\gamma_2 - \gamma_1 - \gamma_3)$$

$$+ \sum_{j=1}^{3} \alpha_{e2j} a_2 a_j^2 = 0, \tag{11d}$$

$$2\omega_3(\zeta_3 a_3 + a_3') - \tfrac{1}{2} f_{31} a_1 \sin(\gamma_1 + \gamma_3) + \tfrac{1}{4} Q_7 a_2 a_1^2 \sin(\gamma_3 - \gamma_2 - 2\gamma_1)$$

$$+ \tfrac{1}{4} Q_8 a_2^2 a_1 \sin(\gamma_1 + \gamma_3 - 2\gamma_2) = 0, \tag{11e}$$

$$2\omega_3 a_3(\gamma_3' - \sigma_{e3}) - \tfrac{1}{2} f_{31} a_1 \cos(\gamma_1 + \gamma_3) + \sum_{j=1}^{3} \alpha_{e3j} a_3 a_j^2 + \tfrac{1}{4} Q_7 a_2 a_1^2 \cos(\gamma_3 - \gamma_2 - 2\gamma_1)$$

$$+ \tfrac{1}{4} Q_8 a_2^2 a_1 \cos(\gamma_1 + \gamma_3 - 2\gamma_2) = 0, \tag{11f}$$

where

$$\gamma_n = -\beta_n + \sigma_{en} T_1, \quad \sigma_{e1} = (\sigma_2 + 0{\cdot}5\sigma_1)/3,$$

$$\sigma_{e2} = 0{\cdot}5\sigma_1, \quad \sigma_{e3} = -\sigma_3 + (5/3)\sigma_2 + (5/6)\sigma_1.$$

The above equations are known as the *reduced equations*. For steady state, $a_i' = \gamma_i' = 0$, $i = 1, 2, 3$. Thus, we have a set of non-linear algebraic equations which is solved numerically to obtain the fixed-point response of the system. The first order solution of the system can be given by

$$u_n = a_n \cos\{(\omega_n + \varepsilon\sigma_{en})\tau - \gamma_n\}. \tag{12}$$

2.3. STABILITY EQUATIONS OF STEADY STATE RESPONSE

By directly perturbing the reduced equations, one can study the stability of the non-trivial steady state solution. But, as the reduced equations (11) have the coupled terms $a_n\gamma_n'$ ($n = 1, 2, 3$), the perturbed equations will not contain the perturbations $\Delta\gamma_i'$ ($i = 1, 2, 3$) for trivial solutions and hence the stability of the trivial state cannot be studied by directly perturbing equation (11). To circumvent this difficulty, normalization method is adopted by introducing the transformation

$$p_i = a_i \cos\gamma_i, \qquad q_i = a_i \sin\gamma_i, \quad i = 1, 2, 3 \tag{13}$$

into equation (11). Carrying out trigonometric manipulations, one arrives at the following *normalized reduced equations* or the *Cartesian form of modulation equations.*

$$2\omega_1(p_1' + \zeta_1 p_1 + \sigma_{e1} q_1) - \frac{1}{2} f_{13} q_3 - \frac{1}{4}\sum_{i=1}^{3} \alpha_{1j} q_1 (p_j^2 + q_j^2)$$
$$+ \frac{1}{4} Q_1 (2p_1 q_1 p_2 - p_1^2 q_2 + q_1^2 q_2) + \frac{1}{4} Q_2 \{p_3(q_1 p_2 + p_1 q_2) + q_3(q_1 q_2 - p_1 p_2)\}$$
$$+ \frac{1}{4} Q_3 \{q_3(p_2^2 - q_2^2) - 2p_2 q_2 p_3\} = 0, \tag{14a}$$

$$2\omega_1(q_1' + \zeta_1 q_1 - \sigma_{e1} p_1) - \frac{1}{2} f_{13} p_3 + \frac{1}{4}\sum_{i=1}^{3} \alpha_{1j} p_1 (p_j^2 + q_j^2)$$
$$+ \frac{1}{4} Q_1 \{2p_1 q_1 q_2 + p_2(p_1^2 - q_1^2)\} + \frac{1}{4} Q_2 \{p_3(p_1 p_2 - q_1 q_2) + q_3(p_1 q_2 + q_1 p_2)\}$$
$$+ \frac{1}{4} Q_3 \{p_3(p_2^2 - q_2^2) + 2p_2 q_2 p_3\} = 0, \tag{14b}$$

$$2\omega_2(p_2' + \zeta_2 p_2 + \sigma_{e2} q_2) - \frac{1}{2} f_{22} q_2 - \frac{1}{4}\sum_{i=1}^{3} \alpha_{2j} q_2 (p_j^2 + q_j^2)$$
$$- \frac{1}{4} Q_4 \{q_1(3p_1^2 - q_1^2)\} + \frac{1}{4} Q_5 \{2p_1 p_3 q_1 - q_3(p_1^2 - q_1)\}$$
$$+ \frac{1}{4} Q_6 \{p_3(p_1 q_2 - p_2 q_1) - q_3(p_1 p_2 + q_1 q_2)\} = 0, \tag{14c}$$

$$2\omega_2(q_2' + \zeta_2 q_2 - \sigma_{e2} p_2) - \frac{1}{2} f_{22} p_2 + \frac{1}{4} \sum_{i=1}^{3} \alpha_{2j} p_2 (p_j^2 + q_j^2)$$

$$+ \frac{1}{4} Q_4 \{p_1 (p_1^2 - 3q_1^2)\} + \frac{1}{4} Q_5 \{2p_1 q_1 q_3 + p_3 (p_1^2 - q_1^2)\}$$

$$+ \frac{1}{4} Q_6 \{p_3 (p_1 p_2 + q_1 q_2) + q_3 (p_1 q_2 - q_1 p_2)\} = 0, \tag{14d}$$

$$2\omega_3(p_3' + \zeta_3 p_3 + \sigma_{e3} q_3) - \frac{1}{2} f_{31} q_1 - \frac{1}{4} \sum_{i=1}^{3} \alpha_{3j} q_3 (p_j^2 + q_j^2)$$

$$- \frac{1}{4} Q_7 \{q_2 (p_1^2 - q_1^2) + 2p_1 p_2 q_1\} + \frac{1}{4} Q_8 \{q_1 (p_2^2 - q_2^2) - 2p_1 p_2 q_2\} = 0, \tag{14e}$$

$$2\omega_3(q_3' + \zeta_3 q_3 - \sigma_{e3} p_3) - \frac{1}{2} f_{31} p_1 + \frac{1}{4} \sum_{i=1}^{3} \alpha_{3j} p_3 (p_j^2 + q_j^2)$$

$$+ \frac{1}{4} Q_7 \{p_2 (p_1^2 - q_1^2) - 2p_1 q_1 q_2\} + \frac{1}{4} Q_8 \{p_1 (p_2^2 - q_2^2) + 2q_1 p_2 q_2\} = 0. \tag{14f}$$

Now perturbing the above equations, one obtains

$$\{\Delta p_1', \Delta q_1', \Delta p_2', \Delta q_2', \Delta p_3', \Delta q_3'\}^{\mathrm{T}} = [J_c]\{\Delta p_1, \Delta q_1, \Delta p_2, \Delta q_2, \Delta p_3, \Delta q_3\}^{\mathrm{T}}, \tag{15}$$

where T is the transpose and $[J_c]$ is the Jacobian matrix whose eigenvalues will determine the stability and bifurcation of the system. The stability boundary of the linear system (i.e., the trivial state) can be obtained from the eigenvalues of the matrix $[J_c]$ by letting $p_i = q_i = 0$, $i = 1, 2, 3$.

The first order solution of the system in terms of p_i, q_i ($i = 1, 2, 3$) can be written as

$$u_1 = p_1 \cos \bar{\omega}_1 \tau + q_1 \sin \bar{\omega}_1 \tau, \tag{16a}$$

$$u_2 = p_2 \cos 3\bar{\omega}_1 \tau + q_2 \sin 3\bar{\omega}_1 \tau, \tag{16b}$$

$$u_3 = p_3 \cos 5\bar{\omega}_1 \tau + q_3 \sin 5\bar{\omega}_1 \tau, \tag{16c}$$

where

$$\bar{\omega}_1 = \omega_1 + \varepsilon(\sigma_2 + 0{\cdot}5\sigma_1)/6. \tag{17}$$

3. NUMERICAL RESULTS AND DISCUSSIONS

From equations (12) and (16), it may be noted that for steady state, the response frequencies for the first three modes are *exactly* in the ratio 1 : 3 : 5 irrespective of the frequency of external excitation ϕ and are *independent of the detuning parameter* σ_3.

Before finding the non-linear response of the system with principal parametric resonance of second mode, it is essential to determine the trivial state stability boundary as it predicts the bifurcation parameters at which the equilibrium state of the beam becomes unstable. Figure 2 shows the trivial state stability boundary of the system with $\mu = 4{\cdot}2$, $\beta = 0{\cdot}24$ and

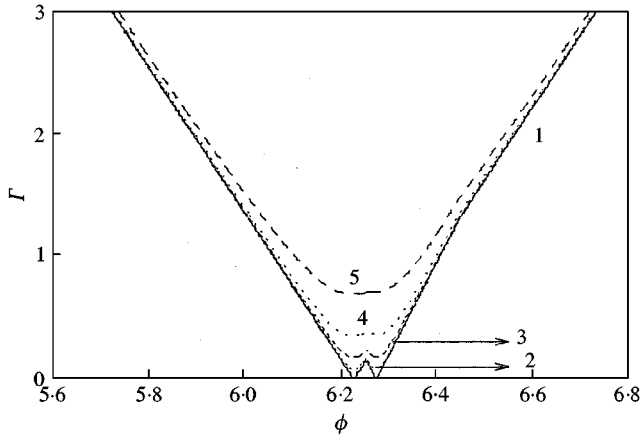

Figure 2. Trivial state stability boundary with 1 : 3 : 5 internal resonance for (1) $\nu = 0{\cdot}001$, (2) $\nu = 2{\cdot}0$, (3) $\nu = 5$, (4) $\nu = 10$, (5) $\nu = 20$.

$J = 0{\cdot}12233$. For low values of damping and forcing parameter (curve 1), the critical points are clearly observed near $\phi = 2\omega_2$ and $\omega_1 + \omega_3$. Here, two zones of instability are observed for low values of Γ and with increase in Γ, these regions merge to form a single unstable region. Curves 2–5 in this figure depict the trivial state instability regions for $\nu = 2$, 5, 10, and 20 respectively. One may note that with a moderate increase in damping, the unstable region remains almost unaltered and with very high values of ν (e.g., $\nu = 20$) not only the width of the unstable region decreases but also the threshold value of instability increases, resulting in the improvement of the stability of the trivial state. For a small change in Γ, the increase in the width of the unstable region in this case is much higher than that of the principal parametric resonance of the first mode with two- [11] and three-mode [28] interactions. Since the system may have stable non-trivial (n-t) fixed-point, periodic, quasi-periodic or even chaotic responses inside this trivial state unstable region, an attempt has been made to explore the possibility of the existence of these responses and study their bifurcation and stability for a wide range of values of the control parameters.

The fixed-point response is obtained by solving numerically the reduced equations (11) and its stability is determined by studying the eigenvalues of the Jacobian matrix J_c. Solid and dotted lines in the response curves, respectively, represent the stable and unstable branches. Figure 3 shows the frequency response curve for $\Gamma = 1$, $\nu = 5{\cdot}0$. The trivial state loses its stability by two subcritical pitchfork bifurcations (PFBs) ($\phi = 6{\cdot}06$ and $6{\cdot}41$). The entire frequency range can be divided into three zones, the first zone being left to the unstable region and the third zone to the right of the unstable one. The unstable region of the trivial branch is the second zone. While in the third zone the response is purely trivial, in the first zone the system has many unstable branches with a stable non-trivial (n-t) and trivial branch. Also, in the first zone, the first- and third-mode fixed-point responses are *quenched* while that of second mode increases with a decrease in the frequency of external excitation ϕ. When one increases the frequency ϕ across the subcritical PFB at $\phi = 6{\cdot}06$ or decreases ϕ across the subcritical PFB at $\phi = 6{\cdot}41$, *blue sky catastrophe* will be observed in the system, as it is attracted by a strange attractor toward a stable fixed point at infinity due to the absence of any deterministic stable attractor in the near vicinity. The n-t stable branch in the first zone loses its stability by subcritical Hopf bifurcation (HB) ($\phi = 6{\cdot}03$) so that the response may jump down from the stable n-t branch to the stable trivial state which becomes unstable at the subcritical PFB($\phi = 6{\cdot}06$).

With decrease in damping [e.g., $v = 2$, Figure 3(b)], while the number of unstable n-t branches increases, that of the stable n-t branches remains unchanged. Also, there is no change in the trivial state PFB points ($\phi = 6{\cdot}06$ and $6{\cdot}41$), but n-t stable branch becomes unstable at $\phi = 6{\cdot}01$. *Hence, with an increase in damping, though the improvement of trivial state stability is marginal, that of the n-t state stability is remarkable.*

For low values of Γ, Figure 4(a) ($\Gamma = 0{\cdot}075$, $v = 2$) shows only the second-mode frequency response curve as the first- and third-mode stable fixed-point responses are *quenched* and

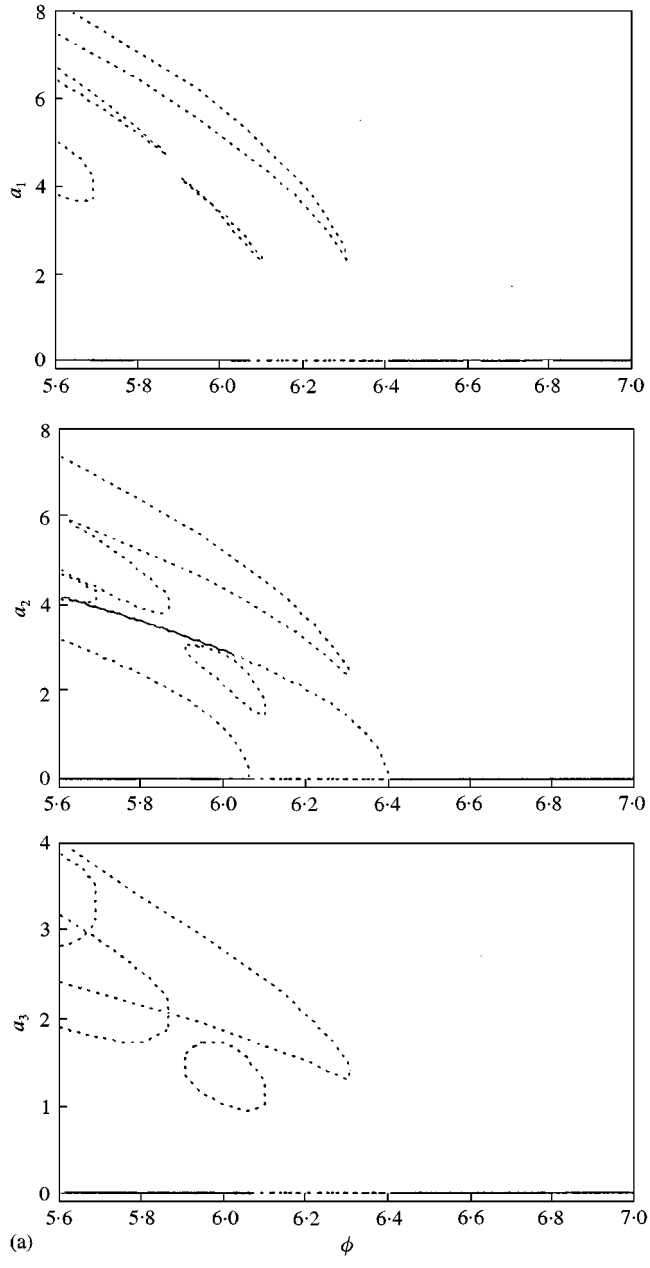

Figure 3. (a) Frequency response curve for $\Gamma = 1{\cdot}0$, $v = 5$; quenching of the first- and third-mode stable fixed point response. (b) Frequency response curve for $\Gamma = 1{\cdot}0$, $v = 2$.

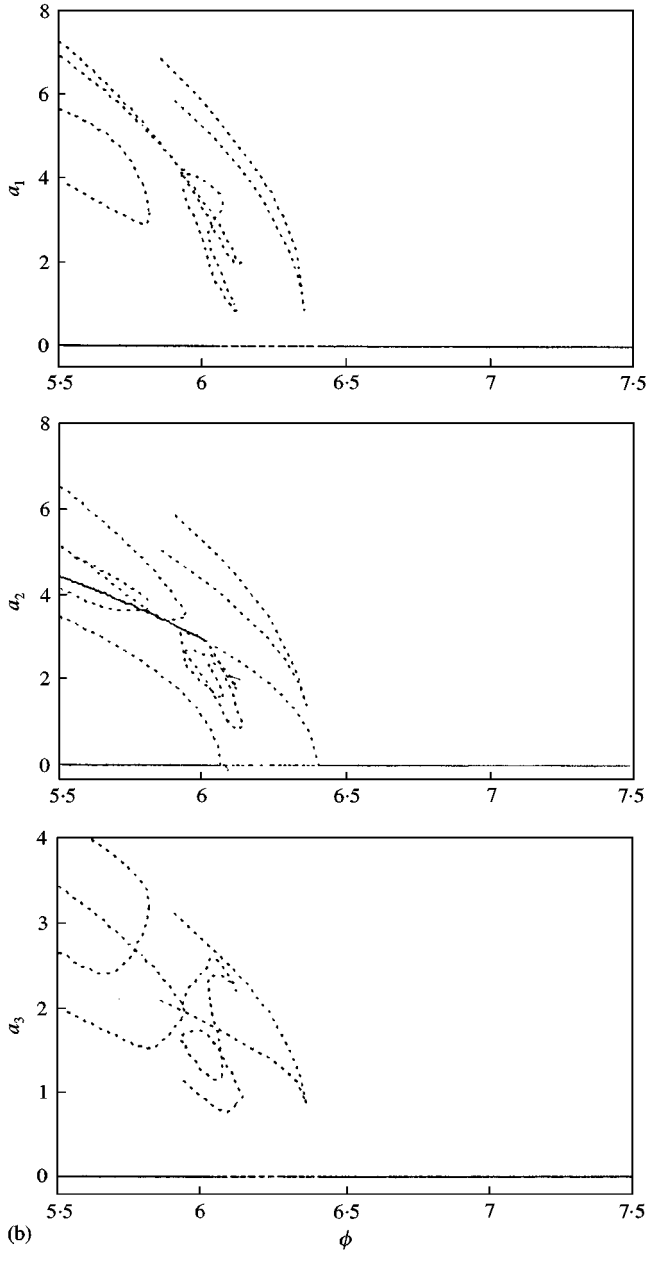

Figure 3. Continued.

the bifurcation points for all the three modes are identical. Here the trivial state has alternate stable and unstable regions with bifurcation points of subcritical PFB ($\phi = 6{\cdot}22$), supercritical PFB ($\phi = 6{\cdot}235$), and supercritical HBPs at $\phi = 6{\cdot}27$ and $6{\cdot}28$. These two HBPs act as the global origins for the periodic responses. One may note that the n-t branch emanating from the supercritical BP is stable and hence, unlike the previous case (Figure 3), here the trajectory will not escape to infinity, but the system will suffer a jump-up phenomena at the subcritical PFB ($\phi = 6{\cdot}22$).

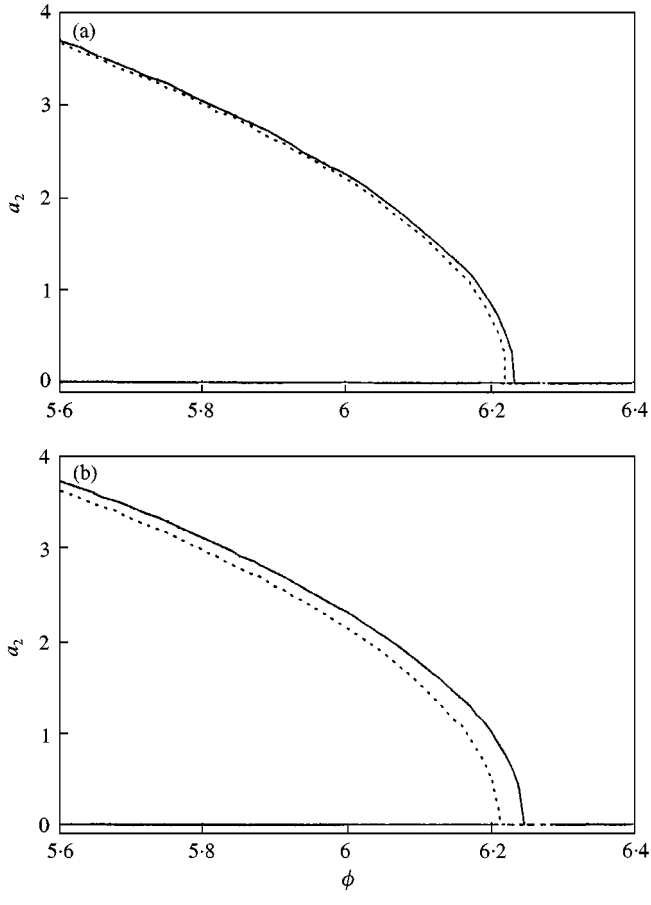

Figure 4. Frequency response curves for second mode with (a) $\Gamma = 0{\cdot}075$, $v = 2$; (b) $\Gamma = 0{\cdot}2$, $v = 5$.

With further increase in v or decrease in Γ, the system will have only the trivial response when the control parameter crosses the threshold value of the trivial state stability. For example, when $\Gamma = 0{\cdot}0075$ and $v = 5$, the system has only a trivial stable branch. Figure 4(b) shows the frequency response of the second mode for $\Gamma = 0{\cdot}2$, $v = 5$, which is topologically equivalent to that of Figure 4(a). Here, the bifurcations occur at $\phi = 6{\cdot}21$ (subcritical PFB), 6·25 (supercritical PFB) and at 6·26 and 6·29 (supercritical HBPs). From Figures 3 and 4, it may be noted that *with an increase in* Γ, *for the same value of* v, *the trivial unstable zones merge and the stable n-t branch becomes unstable by subcritical HB*. For high values of Γ [e.g., $\Gamma = 2{\cdot}5$ (figure not shown)], this n-t branch becomes unstable between two subcritical HBPs.

As topologically equivalent response curves are obtained with variation in the control parameters, it is important to note the change of the bifurcation points with the control parameters so as to avoid the system failure. Figure 5 shows the bifurcation diagram for $v = 5$ where curves 1, 2, 3 and 4 are, respectively, the set of n-t HBP, trivial PFB, supercritical n-t HBP and trivial PFB points. It may be noted that *bistability region* exists to the left of curves 1 and 2, respectively, for the values of control parameters above and below their point of intersection (O). Hence, one may observe jump-up from the trivial state to the n-t stable branch for values of control parameters below O and jump-down from the n-t

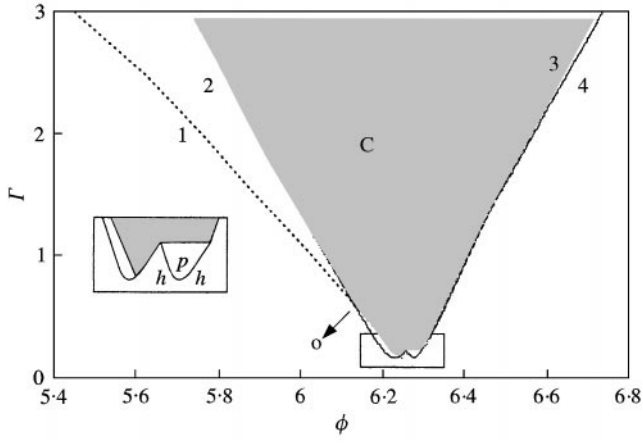

Figure 5. Bifurcation set for $\nu = 5$. Lines 1: n-t subcritical HBP, 2: trivial subcritical PFB, 3: n-t supercritical HBP and 4: trivial supercritical HBP/PFB, C-chaotic, p-periodic, h-supercritical HBPs.

stable branch to the trivial stable branch for the values control parameters above O. While for lower values of Γ, curve 4 is the set of supercritical HBPs, when it meets curve 3 the set of subcritical HBPs, it becomes supercritical PFB. *Hence, one should not operate the system with the values of the control parameters, lying in the shaded area between curves* 2 *and* 3, *as the response is chaotic in this zone.*

The variation of the periodic responses with Γ and ϕ having global origin at the supercritical HBP for $\nu = 2$ is shown in Figure 6. While orbit 1 is drawn for $\phi = 6{\cdot}270$ and $\Gamma = 0{\cdot}2$, orbits 2–4 are plotted for $\Gamma = 0{\cdot}075$ with increasing values of ϕ. Orbits 1 and 2 indicate that, for a higher value of Γ, the periodic response created near the supercritical HBP has a higher response amplitude. It is observed that the periodic orbits created at the supercritical HBP (e.g., $\phi = 6{\cdot}270$, orbit 1) decrease with increase in ϕ and disappear at the other supercritical HBP ($\phi = 6{\cdot}28$). With increase in ϕ (curves 2–4), the response amplitude decreases and the second-mode periodic orbit gets deformed before it disappears at the other supercritical HBP. Though the system undergoes simultaneous resonances of principal parametric of second-mode and combination parametric of $\omega_1 + \omega_3$, the amplitude of the second-mode periodic response is negligible in comparison to those of the first and third modes. This is due to the fact that ϕ, in this case, is closer to $\omega_1 + \omega_3$ than to $2\omega_2$; although the difference of frequencies in these two cases in marginal. Along with these periodic responses, where the system oscillates about the unstable trivial state, there exists another set of periodic responses (Figure 7) where the second-mode response does not oscillate about the trivial state.

As damping increases, these periodic responses disappear when the associated frequency of external excitation falls in the stable zone marked by the trivial state stability boundary. But, with decrease in damping, the system response may be chaotic depending on the amplitude of external excitation Γ.

Figure 8 shows the response obtained by the numerical integration of the temporal equation of motion for different values of ϕ with $\Gamma = 1$ and $\nu = 2$. The time responses Figure 8(a, b) are plotted, respectively, for $\phi = 5{\cdot}5$ and $6{\cdot}5$. Both perturbation result (Figure 3) and numerical integration of the temporal equation indicate the presence of the stable trivial fixed-point response. In Figure 8(c), the time response shows the presence of unstable fixed point at $\phi = 6{\cdot}225$. For the same physical parameters as in Figure 8(c), with another set of initial conditions, the system response is found to be chaotic. Figure 8(d)

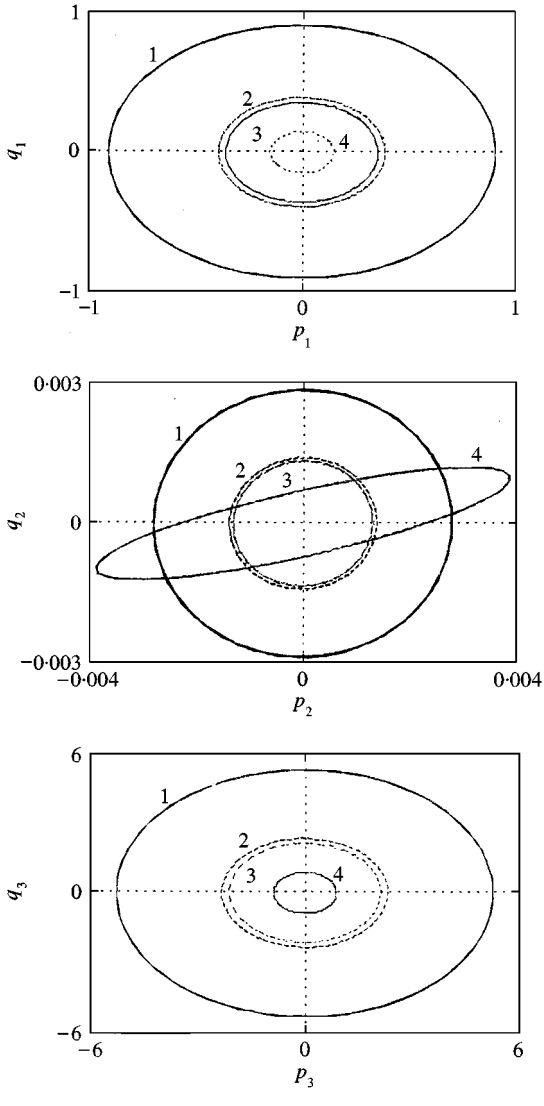

Figure 6. Variation of periodic responses with ϕ and Γ near supercritical HBP. (1) $\phi = 6{\cdot}27$, $v = 2$, $\Gamma = 0{\cdot}2$; $\Gamma = 0{\cdot}075$, $v = 2$: (2) $\phi = 6{\cdot}274$, (3) $\phi = 6{\cdot}278$, (4) $\phi = 6{\cdot}279$.

shows the Poincaré section of this chaotic response. This shows that the prediction of the perturbation results (Figures 2 and 3) are in good agreement with the numerical integration of temporal equation of motion.

Figure 9 shows the time response which consists of laminar stretches of pseudo-quasiperiodic oscillations with interruptions in the form of chaotic bursts for $\phi = 6{\cdot}3$, $\Gamma = 0{\cdot}2$ and $v = 2$. This type of transition to chaos, commonly known as the *type II intermittency* [17], occurred due to the presence of subcritical Hopf bifurcation in the fixed-point response. With decrease in ϕ, the periodic response shown in Figure 10(a, b) for $\Gamma = 0{\cdot}5$, $\phi = 6{\cdot}22$, $v = 7$ becomes chaotic by the *type II intermittency route to chaos*. From the time response (c–e) it is evident that the chaotic outburst irregularly erupts from and returns to or revisits the original periodic response. The phase portraits of this chaotic response is shown in Figure 11 which indicate the chaotic bursts shuttle between the

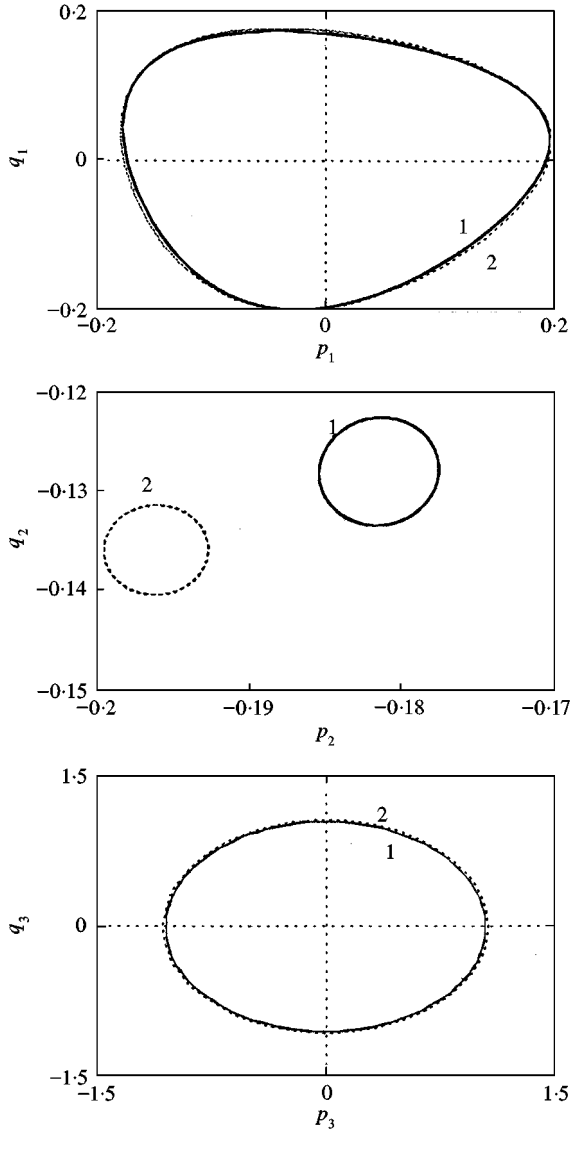

Figure 7. Periodic responses with $\Gamma = 0{\cdot}075$, $v = 2$: (1) $\phi = 6{\cdot}277$, (2) $\phi = 6{\cdot}278$.

unstable non-trivial and trivial fixed points. One may observe that the chaotic outburst is more frequent in this case than the previous one (Figure 9). Hence with an increase in Γ the system becomes more chaotic. Also, the maximum value of the Lyapunov exponents is found to be positive characterizing the response to be chaotic (Figure 8(d)–11).

4. CONCLUSIONS

The non-linear dynamics of a slender beam carrying a lumped mass subjected to a base excitation is studied for principal parametric resonance of second mode which is simultaneously resonated by combination resonance ($\omega_1 + \omega_3$) due to the presence of

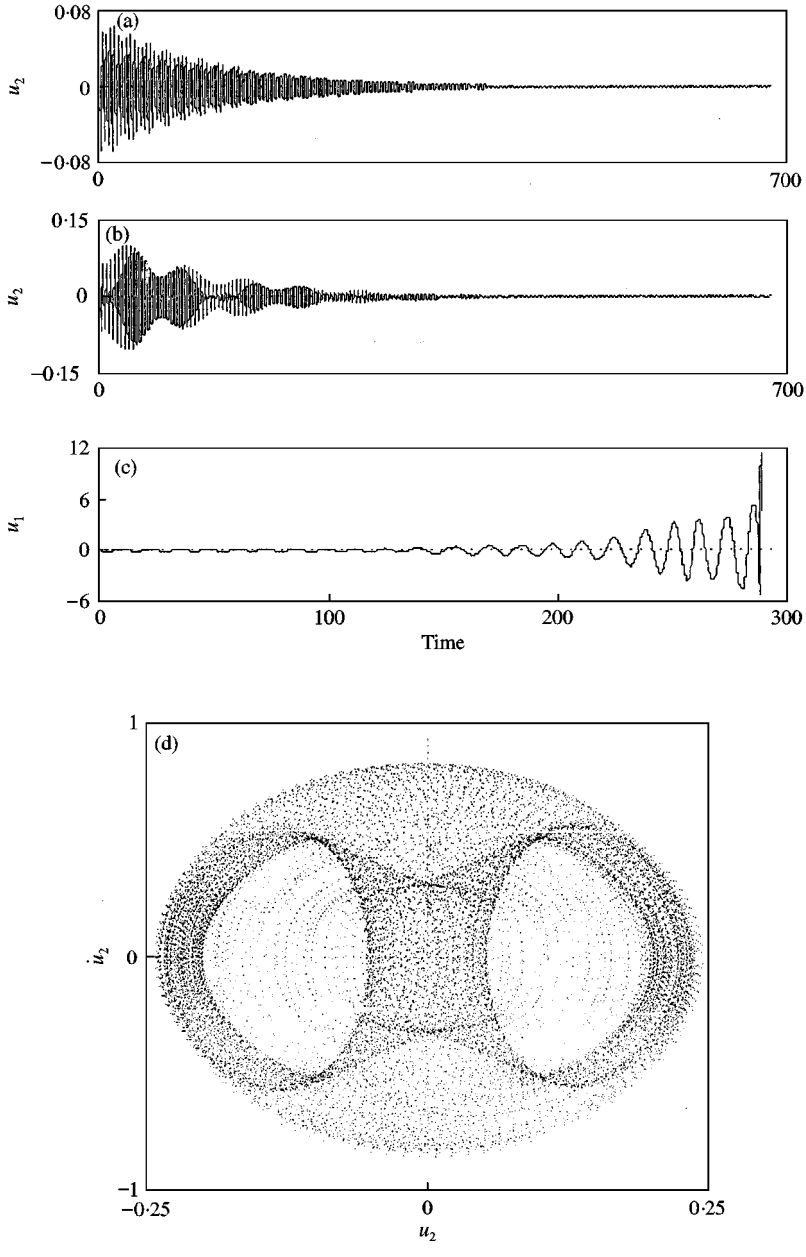

Figure 8. Time spectra and Poincaré section obtained from the numerical integration of the temporal equation of motion with $\Gamma = 1$, $v = 2$; (a) $\phi = 5{\cdot}5$, (b) $\phi = 6{\cdot}5$, (c, d) $\phi = 6{\cdot}225$.

internal resonance of 1 : 3 : 5. Though for lower values of Γ, distinct zones of instability are observed in the trivial state, with increase in Γ, these zones merged to form a single unstable zone with sub- and supercritical pitchfork bifurcations at the ends. The first- and third-mode stable responses are quenched while that of the second mode increases with decrease in the frequency of external excitation. The bifurcations in the non-trivial fixed point branch are subcritical Hopf types. Periodic responses are observed only for lower values of Γ near the unstable zone at $\omega_1 + \omega_3$. With other parameters fixed, a decrease in

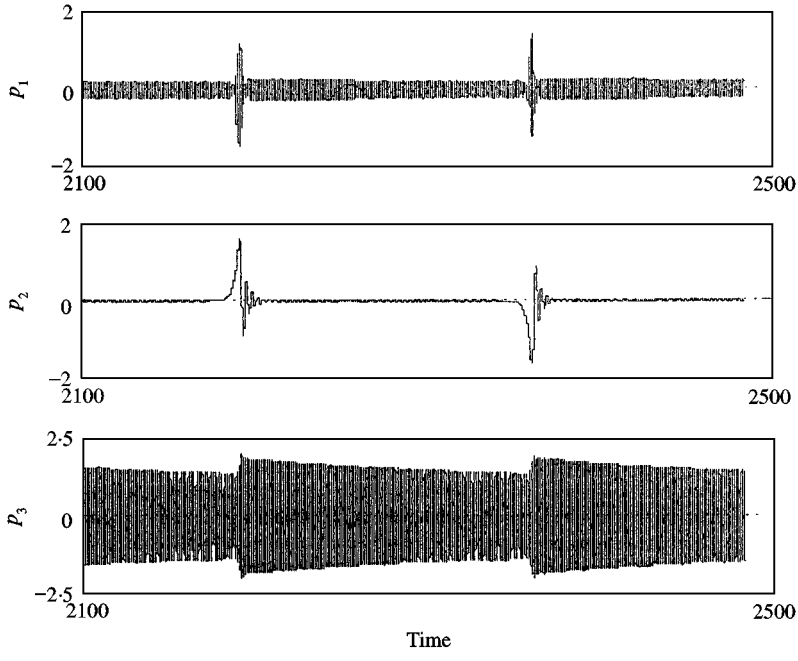

Figure 9. Time spectra showing type II intermittency route to chaos for $\phi = 6{\cdot}3$, $\Gamma = 0{\cdot}2$, $v = 2$.

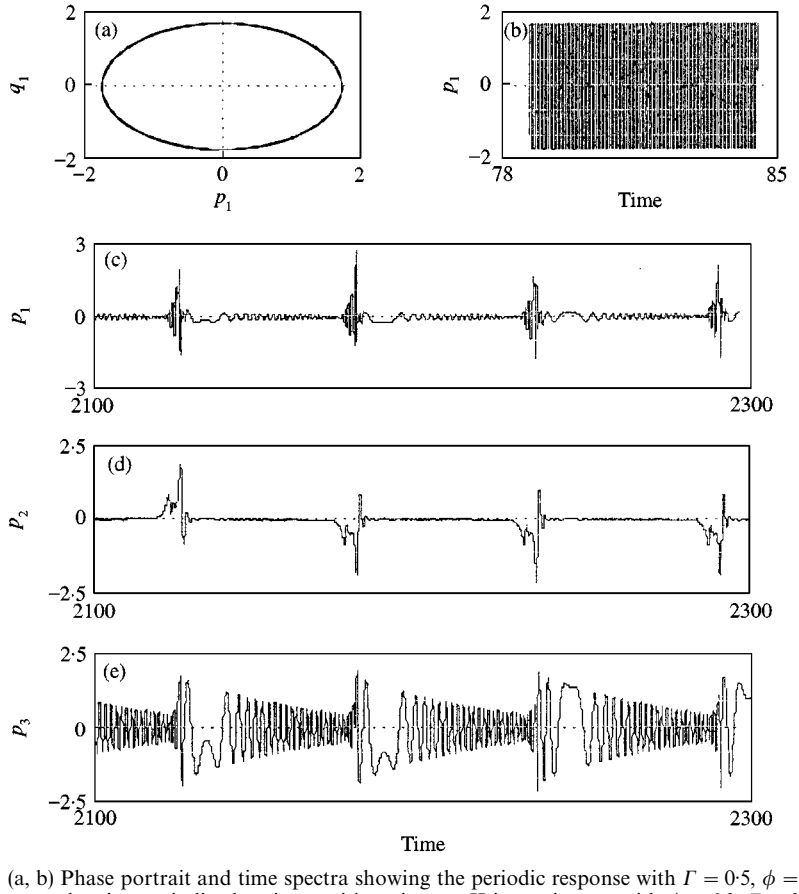

Figure 10. (a, b) Phase portrait and time spectra showing the periodic response with $\Gamma = 0{\cdot}5$, $\phi = 6{\cdot}22$, $v = 7$. (c–e) Time spectra showing periodic-chaotic transition via type II intermittency with $\phi = 6{\cdot}2$, $\Gamma = 0{\cdot}5$, $v = 7$.

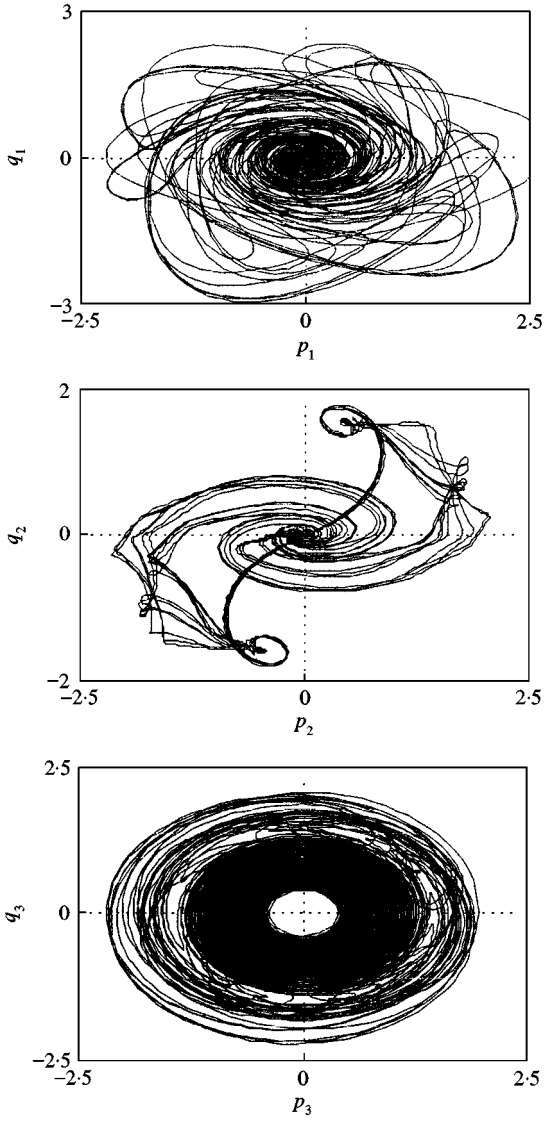

Figure 11. Phase portrait showing the chaotic burst shuttle between the unstable trivial and non-trivial fixed points.

ϕ or an increase in Γ makes the periodic response chaotic through an intermittency route to chaos of type II. The numerical integration of the original temporal differential equation are in good agreement with the perturbation results. The bifurcation set is plotted so that one can visualize the safe zone to avoid a catastrophic failure of the system. Poincaré section and Lyapunov exponents are obtained to verify the chaotic response.

REFERENCES

1. C. W. S. To 1982 *Journal of Sound and Vibration* **83**, 445–460. Vibration of a cantilever beam with a base excitation and tip mass.

2. M. GÜRGÖZE 1986 *Journal of Sound and Vibration* **108**, 73–84. Parametric vibrations of a restrained beam with an end mass under displacement excitation.
3. K. L. HANDOO and V. SUNDARARAJAN 1971 *Journal of Sound and Vibration* **18**, 45–53. Parametric instability of a cantilevered column with end mass.
4. P. A. A. LAURA and R. H. GUTIERREZ 1986 *Journal of Sound and Vibration* **108**, 123–131. Vibrations of an elastically restrained cantilever beam of varying cross section with tip mass of finite length.
5. R. F. FUNG and H. C. CHANG 1998 *Journal of Sound and Vibration* **216**, 751–769. Dynamic modelling of a nonlinearly constrained flexible manipulator with a tip mass by Hamilton's Principle.
6. H. P. LEE 1995 *Journal of Sound and Vibration* **183**, 91–98. Stability of a cantilever beam with tip mass subjected to axial sinusoidal excitations.
7. G. MUSTAFA and A. ERTAS 1995 *Journal of Sound and Vibration* **182**, 393–413. Dynamics and bifurcations of a coupled column-pendulum oscillator.
8. K. SATO, H. SAITO and K. OTOMI 1978 *American Society of Mechanical Engineers, Journal of Applied Mechanics* **45**, 643–648. The parametric response of a horizontal beam carrying a concentrated mass under gravity.
9. H. SAITO and N. KOIZUMI 1982 *International Journal of Mechanical Sciences* **24**, 755–761. Parametric vibrations of a horizontal beam with a concentrated mass at one end.
10. L. D. ZAVODNEY and A. H. NAYFEH 1989 *International Journal of Non-linear Mechanics* **24**, 105–125. The nonlinear response of a slender beam carrying a lumped mass to a principal parametric excitation: theory and experiment.
11. R. C. KAR and S. K. DWIVEDY 1999 *International Journal of Nonlinear Mechanics* **34**, 515–529. Nonlinear dynamics of a slender beam carrying a lumped mass with principal parametric and internal resonances.
12. S. K. DWIVEDY and R. C. KAR 1999 *Journal of Sound and Vibration* **221**, 823–848. Dynamics of a slender beam with an attached mass under combination parametric and internal resonances, Part I: steady state response.
13. S. K. DWIVEDY and R. C. KAR 1999 *Journal of Sound and Vibration* **222**, 281–305. Dynamics of a slender beam with an attached mass under combination parametric and internal resonances, Part II: periodic and chaotic responses.
14. A. H. NAYFEH and D. T. MOOK 1979 *Nonlinear Oscillations*. New York: Wiley-Inter-science.
15. M. CARTMELL 1990 *Introduction to Linear, Parametric and Nonlinear Vibrations*. London: Chapman & Hall.
16. W. SZEMPLIŃSKA-STUPNICKA 1990 *The Behaviour of Nonlinear Vibrating Systems*, Vols. 1 and 2. Dordrecht: Kluwer.
17. A. H. NAYFEH and B. BALACHANDRAN 1995 *Applied Nonlinear Dynamics*. New York: Wiley-Interscience.
18. G. IOOSS and D. D. JOSEPH 1980 *Elementary Stability and Bifurcation Theory*. New York: Springer-Verlag.
19. S. CHOW and J. K. HALE 1982 *Methods of Bifurcation Theory*. New York: Springer-Verlag.
20. Y. A. KUZNETSOV 1995 *Elements of Applied Bifurcation Theory*. New York: Springer-Verlag.
21. A. H. NAYFEH and P. F. PAI 1989 *International Journal of Non-linear Mechanics* **24**, 139–158. Non-linear non-planar parametric responses of an in-extensional beam.
22. E. G. TEZAK, D. T. MOOK and A. H. NAYFEH 1978 *Transactions of the American Society of Mechanical Engineers, Journal of Machine Design* **100**, 651–655. Nonlinear analysis of the lateral response of columns to periodic loads.
23. A. H. NAYFEH 1983 *Journal of Sound and Vibration* **88**, 547–557. The resonance of two degree-of-freedom systems with quadratic nonlinearities to parametric excitation.
24. A. H. NAYFEH 1983 *Journal of Sound and Vibration* **90**, 237–244. The response of multi-degree-of-freedom systems with quadratic nonlinearities to a harmonic parametric resonance.
25. S. L. BUX and J. W. ROBERT 1986 *Journal of Sound and Vibration* **104**, 497–520. Non-linear vibratory interactions in systems of coupled beams.
26. R. P. ASHWORTH and A. D. S. BARR 1987 *Journal of Sound and Vibration* **118**, 47–68. The resonances of structures with quadratic inertial nonlinearity under direct and parametric harmonic excitation.
27. A. H. NAYFEH and B. BALACHANDRAN 1989 *American Society of Mechanical Engineers, Applied Mechanics Reviews* **42**, S175–S201. Modal interactions in dynamical and structural systems.

28. S. K. DWIVEDY and R. C. KAR *International Journal of Non-linear Mechanics* Nonlinear dynamics of a slender beam carrying a lumped mass under principal parametric resonance with three-mode interactions (in press).
29. T. A. NAYFEH, A. H. NAYFEH and D. T. MOOK 1994 *Nonlinear Dynamics* **6**, 353–374. A theoretical and experimental investigation of three-degree-of-freedom structure.
30. W. K. LEE and C. H. KIM 1995 *American Society of Mechanical Engineer*, *Journal of Applied Mechanics* **62**, 1015–1022. Combination resonances of a circular plate with three mode interaction.

APPENDIX A

The expressions for the terms Q_n are given by

$$\begin{aligned}
Q_1 &= \alpha^1_{112} + \alpha^1_{121} + \alpha^1_{211} + \omega_1^2\beta^1_{211} - \omega_1\omega_2(\beta^1_{121} + \beta^1_{112}) \\
&\quad - \{\omega_1^2(\gamma^1_{211} + \gamma^1_{121}) + \omega_2^2\gamma^1_{112}\}, \\
Q_2 &= \alpha^1_{123} + \alpha^1_{132} + \alpha^1_{213} + \alpha^1_{231} + \alpha^1_{312} + \alpha^1_{321} \\
&\quad - \omega_1\omega_2(\beta^1_{312} + \beta_{321}) + \omega_1\omega_3(\beta^1_{231} + \beta^1_{213}) \\
&\quad + \omega_2\omega_3(\beta^1_{123} + \beta_{132}) - \omega_1^2(\gamma^1_{321} + \gamma^1_{231}) \\
&\quad - \omega_2^2(\gamma^1_{132} + \gamma^1_{312}) - \omega_3^2(\gamma^1_{123} + \gamma^1_{213})\}, \\
Q_3 &= \alpha^1_{223} + \alpha^1_{232} + \alpha^1_{322} - \omega_2^2\beta^1_{322} + \omega_1\omega_2(\beta^1_{223} + \beta^1_{232}) \\
&\quad - \{\omega_2^2(\gamma^1_{232} + \gamma^1_{322}) + \omega_3^2\gamma^1_{223}\}, \\
Q_4 &= \alpha^2_{111} - \omega_1^2(\beta^2_{111} + \gamma^2_{111}), \\
Q_5 &= \alpha^2_{311} + \alpha^2_{131} + \alpha^2_{113} - \omega_1^2\beta^2_{311} + \omega_1\omega_3(\beta^2_{131} + \beta^2_{113}) \\
&\quad - \{\omega_1^2(\gamma^2_{311} + \gamma^2_{131}) + \omega_3^2\gamma^2_{113}\}, \\
Q_6 &= \alpha^2_{312} + \alpha^2_{132} + \alpha^2_{321} + \alpha^2_{123} + \alpha^2_{213} + \alpha^2_{231} \\
&\quad + \omega_1\omega_2(\beta^2_{312} + \beta^2_{321}) - \omega_1\omega_3(\beta^2_{231} + \beta^2_{213}) \\
&\quad + \omega_2\omega_3(\beta^2_{123} + \beta^2_{132}) - \omega_1^2(\gamma^2_{321} + \gamma^2_{231}) \\
&\quad - \omega_2^2(\gamma^2_{132} + \gamma^2_{312}) - \omega_3^2(\gamma^2_{123} + \gamma^2_{213})\}, \\
Q_7 &= \alpha^3_{112} + \alpha^3_{121} + \alpha^3_{211} + \omega_1^2\beta^3_{211} - \omega_1\omega_2(\beta^3_{121} + \beta^3_{112}) \\
&\quad - \{\omega_1^2(\gamma^3_{211} + \gamma^3_{121}) + \omega_2^2\gamma^3_{112}\}, \\
Q_8 &= \alpha^3_{221} + \alpha^3_{212} + \alpha^3_{122} \\
&\quad - \omega_1^2\beta^3_{211} + \omega_1\omega_2(\beta^3_{121} + \beta^3_{112}) \\
&\quad - \{\omega_1^2(\gamma^3_{211} + \gamma^3_{121}) + \omega_2^2\gamma^3_{112}\},
\end{aligned}$$

where α^n_{klm}, β^n_{klm}, γ^n_{klm} have the same definition as in the Appendix of reference [13].

APPENDIX B: NOMENCLATURE

a_n	response amplitude of the nth mode
c	coefficient of damping
d	position of the attached element from the base (Figure 1)
E	Young's modulus of the beam material
f_{nm}	forcing parameter in nth mode due to interaction of the mth mode
g	acceleration due to gravity
I	moment of inertia of the beam section
J	non-dimensional moment of inertia of the attached mass about its centroidal axis perpendicular to $X-Y$ plane
J_0	moment of inertia of the attached mass about its centroidal axis perpendicular to $X-Y$ plane
L	length of the beam
m	mass of the attached element
r	scaling factor
s	reference variable along the beam
t	time
u_n	time modulation of the nth mode
v	lateral displacement of the beam
z	vertical base excitation
Z_0	amplitude of base excitation in mm
Z_r	reference amplitude of base excitation in mm
τ	non-dimensional time
ϕ	non-dimensional frequency of external excitation
$\psi(x)$	shape function of the nth linear mode
ω_n	non-dimensional frequency of the nth mode
Ω	frequency of the external excitation
$(\ )_t$	$\partial(\ )/\partial t$
$(\ )_s$	$\partial(\ )/\partial s$
$(\dot{\ })$	$\partial(\ )/\partial \tau$